Research on Engineering Structures & Materials
www.jresm.org
Research Group

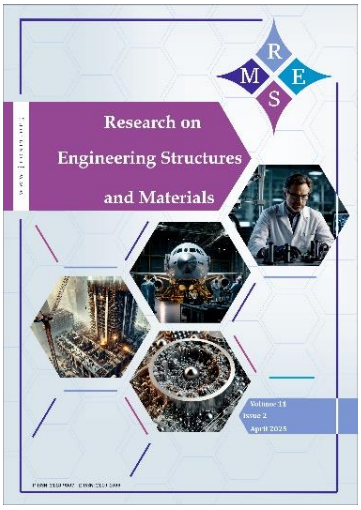

Nonlinear numerical analysis of concrete members subjected to temperature-induced volumetric changes

Ahmad Abdelwahab, Mahmoud El-Kateb, Nabil A. Fouad, Amr Abdelrahman

Online Publication Date: 10 March 2026

URL: http://www.jresm.org/archive/resm2026-1383ma1129rs.html
DOI: http://dx.doi.org/10.17515/resm2026-1383ma1129rs

Journal Abbreviation: *Res. Eng. Struct. Mater.*

To cite this article
Abdelwahab A, El-Kateb M, Fouad N A, Abdelrahman . Nonlinear numerical analysis of concrete members subjected to temperature-induced volumetric changes. *Res. Eng. Struct. Mater.*, 2026; 12(4): 2607-2621.

Research on Engineering Structures & Materials
www.jresm.org

Research Article

Nonlinear numerical analysis of concrete members subjected to temperature-induced volumetric changes

Ahmad Abdelwahab [*1,a], Mahmoud El-Kateb [1,b], Nabil A. Fouad [2,c], Amr Abdelrahman [1,d]

[1]*Structural Engineering Department, Faculty of Engineering, Ain Shams University, Egypt*
[2]*Institute of Building Physics, Leibniz University Hannover, Germany*

Article Info

Article History:

Received 29 Nov 2025

Accepted 08 Mar 2026

Keywords:

Concrete damaged plasticity; Cracking-induced stiffness reduction; Nonlinear finite element analysis; Reinforced concrete; Thermo-mechanical coupling, Volumetric changes

Abstract

The present paper investigates the capability of Nonlinear Finite Element Analysis (NLFEA) in predicting the behavior of Reinforced Concrete (RC) members subjected to combined gravity and temperature loads. The experimental and NLFEA results show that temperature changes have notable influence on the initiation of cracking, the stiffness degradation and ultimate load-carrying capacity. The NLFEA outcomes were compared to the experimental data of RC beams subjected to uniform and through-thickness temperature gradients. The NLFEA modelling technique, presented in this paper, reasonably well simulated the load–displacement history, cracking patterns and failure modes. Cracking loads and ultimate capacities for all tested specimens were estimated within 10% of the experimental data. In some cases, there was a slight overprediction of cracking loads and slight under-prediction of ultimate strengths; however, the agreement was generally consistent. Mesh sensitivity studies proved that the NLFEA solution converged and showed more accurate results as the discretization is refined. The conclusions emphasize the significance of considering nonlinear material behavior, tension stiffening and differential thermal expansion of steel and concrete for the thermo-mechanical analysis. In summary, the results indicate that the proposed NLFEA model offers a robust and accurate prediction of RC structural behavior under combined thermal and gravity loading.

1. Introduction

For RC members experiencing volumetric changes, structural behavior of such members is controlled by the extent and pattern of cracking [1-6]. Stiffness and stress-carrying capacity of the section drops off when cracking takes place; therefore, cross-sectional area contributes to some extents to carrying internal forces. Therefore, the correct calculation of volumetric change-induced stress must take this stiffness reduction into account. Herein, the area stiffness is modified during FEA in the linear analysis. If a completely uncracked section is assumed the stress level overestimate is obtained, and this influences incorrectly the reliability of internal force estimate.

Hence, it is important to estimate the effective section properties with care to obtain accurate results. Modulus of elasticity is an important property of concrete in determining the stress–strain behavior. Once the cracking sets in, this relation ceases to be linear [3-7]. The combination of volumetric change and stiffness reduction leads to effective values of structural deformation and internal stresses non-identical with those at elastic stage. This interaction is very important for correct structural evaluation and better performance prediction and design options.

*Corresponding author: ahmad.tarek@eng.asu.edu.eg
[a]orcid.org/0009-0009-0548-735X; [b]orcid.org/0000-0001-6189-7200; [c]orcid.org/0000-0002-0962-8262; [d]orcid.org/0000-0002-8844-7039
DOI: http://dx.doi.org/10.17515/resm2026-1383ma1129rs

Effect of temperature fluctuations becomes more significant in flat slabs and the other long span systems [12,14]. Induced axial forces affect both flexural and shear action. At present, design codes or standards [17-22] give provisions to adjust one-way shear strength due to axial force influence. This is accounted for by recognizing that compression increases and tension decreases shear strength. However, limited recommendations are available in codes and standards with respect to this effect on the two-way shear resistance. This is a limitation in the literature, for overlong concrete structures under combined load conditions including gravity loads and volumetric variations.

Although international code provisions are available for thermal analysis, the guidelines provided of these codes for RC and prestressed concrete structures are still limited. Current design guidelines show significant degree of variation in the stiffness modification factors and do not include a coherent structure for simulating thermally induced volumetric variations. Moreover, the existing provisions do not present a comprehensive or systematic approach to combine thermal actions and mechanical loads in restrained members where internal force redistribution controls the behavior. Furthermore, the assumption of simplified or nominal temperature distribution through member thickness introduces an error in predicted thermal stresses. Further, present codes do not adequately differentiate between the essentially different thermal reactions of RC and prestressed concrete, with reference to prestress loss effects, cracking control and serviceability issues. These gaps reveal that current code-based requirements are inadequate for accurate prediction of the thermal response and resilient performance, suggesting the need for a more comprehensive and systematically validated framework.

The crack initiation and shear failure in the interface were caused by early uniaxial tensile stress, as observed from the literature, whereas axial compressive stress retarded cracking. However, the majority of such understandings are about one-way shear and two-way shear behavior under an axial load is still not well understood. Paucity of comprehensive provisions on such retrofit measures in codes and standards like ACI, Eurocode, and ECP indicates the pressing need for more experimental as well as numerical studies. And besides the changing volumes, this extended structural continuity has structural implications. Elimination of expansion joints can improve the symmetry and efficiency in lateral load-resisting systems. When the expansion joints divide the structure, they may result in non-symmetric stiffness distribution and consequently decrease seismic response of whole buildings as well as a winded loading capacity. This can be explained schematically through Fig. (1). On the other hand, no knot in a joint-free setting implies more regular behavior and better robustness. But this strengthened mechanical stability must be weighed against the elevated volumetric changes at the system.

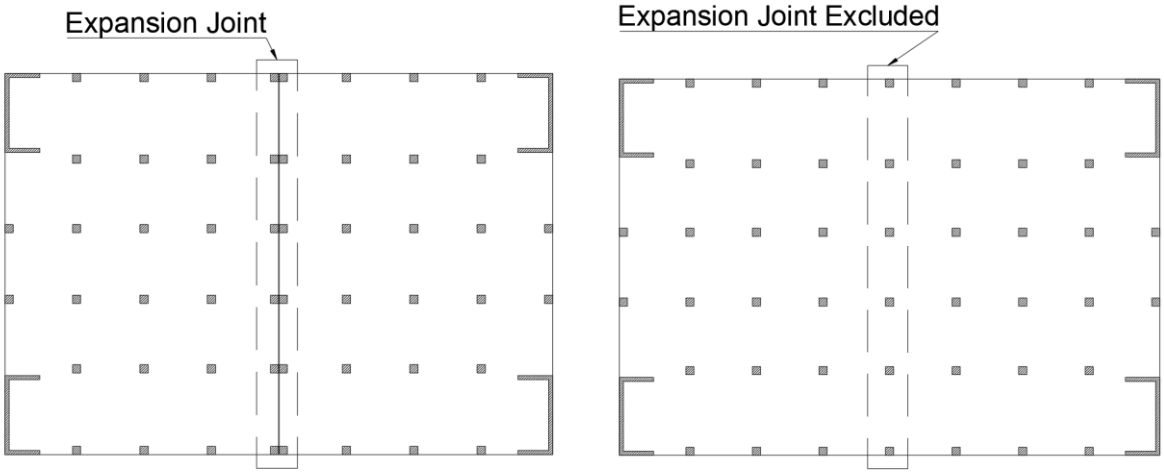

(a) (b)

Fig. 1. (a) A structure with unsymmetric lateral force resisting system due to the presence of expansion joint, (b) A structure with symmetric lateral force resisting system after exclusion of expansion joint

1.1 Research Objectives

This study highlights the necessity of considering material nonlinearity. Once cracked the internal distribution of forces and structural behavior both under gravity loads as well as volumetric changes are fundamentally different. The main aim of this study is to develop a validated NLFEA method considering the coupled action of gravity and temperature loading in the RC members. This method attempts to improve the accuracies of stresses and deformations considering thermal effects. Thus, this may lead to better estimates of serviceability and durability for RC structures. The proposed tool is aimed to fill the gap between numerical modelling and practical design. Furthermore, this can help structural engineers to take more effective decisions about the overall thermal performance of RC elements under restrained situations. To offer a better insight into the thermal response of RC members, by explicitly considering the role of concrete cracking and hence reduced effective stiffness, it is worth pursuing a further investigation.

2. Experimental Data

To determine the accuracy and robustness of the developed NLFEA technique performed in this study, a thorough review was carried out for previous experimental investigations concerning the combined action between gravity loads and volumetric changes. These studies give valuable insights to the behavior of concrete members under combined thermal and gravity loading. They present the complex interaction between material cracking and structural capacity. The experimental programs presented in previous research serve as an important foundation for analyzing the predictive capability of the numerical models developed throughout this study. Correspondingly, the main observations, behavior, and failure characteristics derived from these experimental tests are combined and presented in the following section for comparison with the NLFEA results of this paper. The selected experimental data capture the dominating thermo-mechanical mechanisms which control the structural response. These studies investigated both uniform temperature variations across concrete sections as well as the effect of temperature gradient. Accordingly, experimental tests represent an ideal benchmark for the performance of numerical models in simulating temperature-induced changes and load carrying capacity.

2.1 DeRosa et al.

DeRosa et al. [8] performed an experimental investigation to investigate the influence of temperature variations on RC members. The study was based on stiffness, strength and crack width against temperature changes. It also studied the mechanical performance of RC beams under freeze–thaw cycles and low temperatures. The testing facility for all experiments was a temperature-controlled room with load frame. The tests were done to study the behavior of RC elements under axial tension in addition to thermal cycles. The specimens tested were full-size RC beams subjected to different temperatures. Four beams with the dimensions of 200 mm × 400 mm ×4200 mm and span length of 3400 mm were tested under four-point bending. Two of the beams were tested at room temperature (+21 °C) and two to (−20°C). Beams 1 and 3 were without shear Reinforcement. Stirrups placed at 175 mm spacing were provided in beams 2 and 4. Loading sequence of the four specimens is illustrated in Table (1).

Table 1. Loading sequence of DeRosa et al. specimens [8]

Beam Number	Stirrups Layout	Load (kN)				Exposure
		Initial Loading	Sustained 48h	Cyclic (5 Cycles)	Final Static	
1	No stirrups	0 - 75	90	75 – 50 - 75	75 up to failure	$-20^{0}C$
2	With Stirrups	0 - 75	90	75 – 50 - 75	75 up to failure	$-20^{0}C$
3	No stirrups	0 - 75	90	75 – 50 - 75	75 up to failure	$+21^{0}C$
4	With Stirrups	0 - 75	90	75 – 50 - 75	75 up to failure	$+21^{0}C$

2.2 Mirzazadeh et al.

Mirzazadeh et al. [9] experimental studied the static performance of RC beams under thermal gradient field through the depth. These differentials were to represent actual conditions of thermal exposure, most pertinent being structures of bridges. The test program included experimentations with four full scale RC beams. The four-step loading sequence was applied to each of the beams. In the first stage, a static load was gradually increased to 90 kN. This load was maintained for 48 h. Then ten loading cycles were performed from 50 kN to 90 kN. Each beam was then tested to failure. The specimens had the same geometry as used by DeRosa et al. [8]. But in contrast to the previous experiment, these beams were not subjected to only horizontal temperature gradients. Loading sequence for the four specimens is illustrated in Table (2). The shear reinforcement and the test temperature state already reflected in being included on the beam's labels. "NS" denotes specimens with no shear reinforcement and "WS" denotes specimens with shear reinforcement. Likewise, "R" is for testing at room temperature (+15°C) and "L" is for low temperature (-25°C). To resist shear, 10M stirrups at 175 mm centers were used in beams WSR and WSL. Contrastingly, NSR and NSL did not contain any shear reinforcement except the minimum stirrups at center of span and supports needed for construction. The four-point bending configuration was used to test all specimens. Heating pads were used on the upper side of each beam. This technique achieved the desired temperature gradient across the depth of the beam.

Table 2. Loading sequence of Mirzazadeh et al. specimens [9]

Beam Description	Beam ID	Load (kN)				Exposure
		Static	Sustained 48h	Cyclic (10 Cycles)	Final Static	
No Shear RFT Room Temp.	NSR	0 - 90	90	90 – 50 - 90	90 up to failure	$+15^{0}$C
No Shear RFT Low Temp.	NSL	0 - 90	90	90 – 50 - 90	90 up to failure	-25^{0}C
With Shear RFT Room Temp.	WSR	0 - 90	90	90 – 50 - 90	90 up to failure	$+15^{0}$C
With Shear RFT Low Temp.	WSL	0 - 90	90	90 – 50 - 90	90 up to failure	-25^{0}C

3. Nonlinear Finite Element Analysis

This research provides a numerical study on the behavior of concrete beams and long-span RC members under combined gravity-temperature loading. The investigation specifically addresses the volumetric changes due to daily and seasonal environmental processes. These are volumetric variations that can have considerable effect on the performance of overlong members and as such must be analyzed. The primary goal is to study the interaction between volumetric changes and gravity loads, and how the interaction would influence deformation of, cracking in, as well as global stability of a structure. The structural response of RC beams subjected to combined thermal and gravity loading was modelled using NLFEA. Modelling consisted of material definition, imposition of boundary conditions and a sequentially coupled thermal-stress analysis to account for temperature effects. Fig. (2) shows depiction of the created NLFEA models presenting the geometry and arrangement of reinforcement. This figure gives a graphical illustration of the numerical modelling technique. Fig. (2) shows four-point bending configuration. The ends of the specimen were modelled to simulate the support conditions in the experiments. Translation restraints were assigned according to the same conditions applied during testing. Also, two loading points were imposed to apply at them the concentrated loads as applied in experimental testing. All interface conditions and impositions in the NLFEA were made to be consistent with those in experimental setup. A simplified illustration of the supports, load positions, and direction is shown in Fig. (2) for clarity.

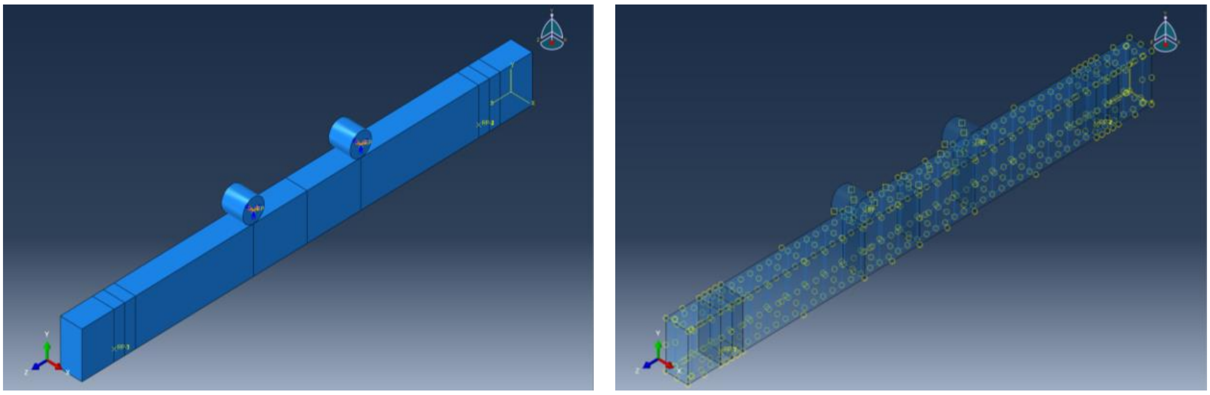

(a) (b)

Fig. 2. (a) 3D Model for RC Beam using ABAQUS/CAE, (b) Embedded Element Technique for Reinforcement inside RC Beam

3.1 Numerical Analysis Parameters

NLFEA was conducted using ABAQUS/CAE. RC members were simulated under combined effect of the gravity and the temperature loads. Concrete was modelled by the C3D8RT 3D continuum solid element, which also enables to perform the accurate thermal and structural behavior simulation [16]. The reinforcement bars were simulated as T3D2 trusses incorporated in the volume of concrete [16]. The reinforcement was embedded in the concrete. The approach allows the steel bars to deform compatibly and in a compatible manner with the adjacent concrete, without requiring an additional interface model. It limits relative steel and concrete sliding for accurate stress transfer and composite action. This approach also simplifies the meshing by eliminating the requirement for shared or coincident nodes at interface travel. Hence, it makes the model simplified and retains the numerical accuracy. The thermal expansions of concrete and steel were defined with different values, which allows the model to calculate internal stresses due to thermally induced expansion differences between both materials.

3.1.1 Sequentially Coupled Thermal-Stress Analysis

A sequential thermal-stress analysis was employed to model the behavior of RC members subjected to biaxial loading. This approach consists of two separate computation steps. First, the temperature distribution in the member is calculated. Step also includes the thermal properties of concrete and steel, as well as the boundary conditions and environmental effects including ambient temperature and solar radiation. The emerging temperature field is subsequently provided as an input for the structural analysis. In the second step, the defined temperature field is applied to the structural model. This step calculates the stress and strain responses of RC member under the interaction between mechanical and volumetric quantities. The temperature change causes thermal expansion or contraction, resulting in thermoelastic strains. Such strains are superimposed on those due to external action from gravity loads, causing redistribution of stresses in the element.

3.2 Concrete Material Model

The CDP model is chosen for this study because it offers the best flexibility and accuracy. CDP model has several beneficial properties, as they include broader mechanical behavior of concrete. It can handle virtually unlimited loading and boundary conditions (monotonic, cyclic, dynamic), which make it become a versatile tool in both nonlinear structural analyses. It allows detailed description of concrete behavior under mechanical and volumetric loading necessary the assessing structural condition in open environment. To accurately simulate the material nonlinearity of concrete, especially in compression, the Modified Hognestad model [23] was used. In this model, the classical Hognestad curve is further developed by giving a more detailed representation of both ascending and descending branches on the stress-strain curve. In the pre-peak zone, the model expresses compressive stress (fc) as a parabolic function of strain ε_c according to Eq. (1), which is satisfied up to the peak condition for compressive strain (εc0), that indicates the greatest capacity to resist stress status (fc'). The parameters that are considered for Modified Hognestad model are shown in Table (3). The formula models that stress must soften up to its maximum, in accordance with the true behavior of concrete under compression. In the post-peak part of the curve for which the strain is larger than (ε_{c0}) and arrives at a crushing strain ε_{cu} = 0.0038, as shown in Eq. [2], similar, descending stress represents material softening [23-24].

This simplified linear softening curve is convenient and realistic for the simulation of decrease in bearing capacity by crushing. By employing the CDP model in conjunction with Modified Hognestad stress-strain relation, this paper accommodates gradual variation of damage and nonlinear material response. In RC members subjected to changeable environmental conditions, the combined effect of mechanical and thermal loads affects structural response which requires an integrated modelling considered as a crucial aspect for accurate prediction of lifecycle behavior. Fig. (3) presents the stress-strain curve for unconfined concrete with modified Hognestad model in compression. Concrete in compression was modeled with a modulus of elasticity (E_c) equal to $4700\sqrt{f_c'}$

$$f_c = f_c' \left[\frac{2 * \varepsilon_c}{\varepsilon_{c0}} - \left(\frac{\varepsilon_c}{\varepsilon_{c0}}\right)^2\right] \tag{1}$$

$$f_c = 0.85 * f_c' \tag{2}$$

Table 3. CDP material model parameters

Dilation Angle (ψ)	Eccentricity (ε)	Stress Ratio (f_{b0}/f_{c0})	Shape Factor (K_c)	Viscosity Parameter (μ)
40	0.1	1.16	0.67	0.005

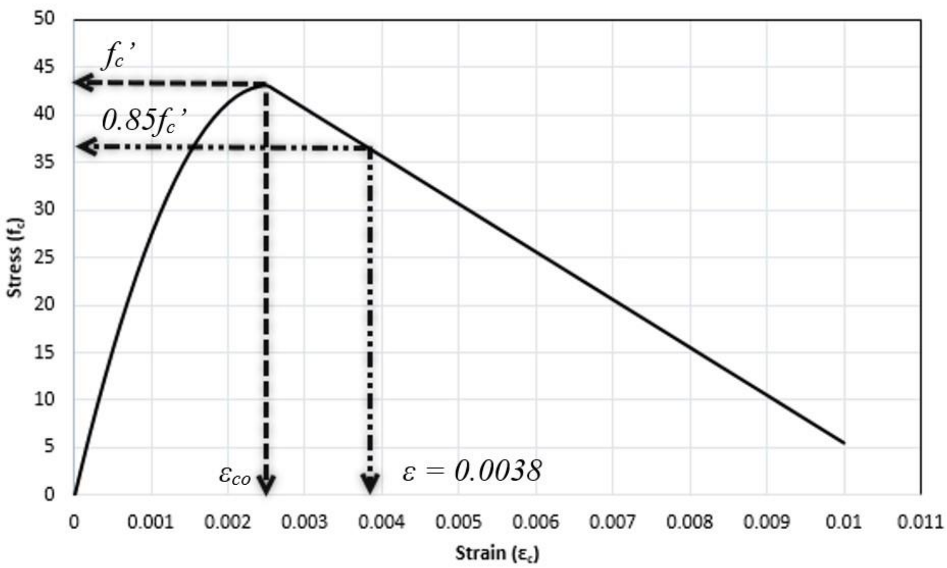

Fig. 3. Stress-strain relationship of concrete in compression using Modified Hognestad model

3.3 Concrete Modulus of Rupture

One of the most important parameters in NLFEA of RC structures is the determination of the direct tensile strength (f_t) of concrete. Researchers and design codes have offered various equations to predict f_t as a function of f_c' [17-22]. For example, ACI 435R-95 [22] proposes Eq. (3) and ACI 318-25 [18] proposes Eq. (4). Several experimental research showed that the tensile strength of concrete is more proximate to the value estimated by ACI 318-25 [18]. This corresponds to a better indication of the resistance of the material against cracking. By contrast, Eq. (3) in ACI 435R-95 [22] is conservative and often results in lower tensile strength. While this more conservative value ensures safety in very uncertain situations or during times aggregates are needed. Hence, considering Eq. (4) in NLFEA simulations of concrete offers a more representative estimation, particularly in the study of crack growing. This is more consistent with what can be observed in the experimental results analyzed within this work. As the use of Eq. (4) in NLFEA would result in more accurate prediction of concrete performance, it will also benefit reliable structural evaluations.

$$f_t = 0.33\sqrt{f_c'} \tag{3}$$

$$f_t = \frac{2}{3} * 0.62\sqrt{f_c'} \tag{4}$$

3.4 Tension Stiffening in Concrete

Exact modeling of tension stiffening is very important for RC members model, where reinforcement is still carrying load after concrete cracks [10]. There are three possible alternatives for modelling concrete tension stiffening. The three alternatives are the stepped response, the stepwise unloading response and the abrupt unloading response. The steplike response divides the stress-strain curve into steps and therefore is computationally easier to analyses. The method described above may, however, fail to properly reflect the viscoelastic nature of tensile behavior in concrete and hence offer less accurate results. The slowly unloading response gives more realistic image, as it presents a smooth continuous decrease in stress with increasing strain past the cracking. This kind of constitutive relationship is closer to the true behavior of concrete in tension but tends to make the modelling and computation more complicated. Finally, the discontinuous unloading response presents itself as an intermediate between both by suffering an immediate decrease of stress but with a behavior more linear. This approach is a compromise between simplicity and accuracy, providing a sharp initial drop while considering extra stress reductions after some higher strain. Although it is more accurate than the stepped response, the partially unloading response may oversimplify some of the features of a fully gradual unloading response. Each approach has advantages and limitations, so the method chosen should depend on a balance between computational simplicity and model accuracy.

Collins-Mitchell approach presents a modified tension stiffening model. This is an extension of the Vecchio-Collins model that includes improvements allowing for a more realistic representation of the interaction between concrete and reinforcement after cracking. The linearity of the stress-strain response is first supposed, by Eq. (5). Where, (f_{cr}) is the tensile stress, (E_c) is the elastic modulus of concrete and (ε_1) is the tensile strain. This is valid until the onset of cracking (ε_{cr}). Beyond this point the nonlinear stress reduction is then applied to simulate a post-cracking response, which is defined by Eq. (6).

$$f_{cr} = E_c\, \varepsilon_1, for\ \varepsilon_1 \leq \varepsilon_{cr} \tag{5}$$

$$f_{ct} = \frac{\alpha_1 \alpha_2\, f_{cr}}{1 + \sqrt{500\varepsilon_1}}, for\ \varepsilon_1 \geq \varepsilon_{cr} \tag{6}$$

The α_1 and α_2 parameters are material dependent constants and commonly found in the literature from testing. The $\sqrt{500\varepsilon_1}$ term thus describes the progressive softening of tensile strength as strain is increased. It represents the asymptotic behavior (when cracks widen and spacing increases, the stress transfer through the concrete matrix is reduced). The Collins-Mitchell model includes contributions from concrete and reinforcement in tension. It discretizes the tension stiffening effect of concrete, that is an interaction between cracked concrete and contained steel. This method enhances the accuracy of numerical estimates of RC structures at service and ultimate loads. With the use of such models, structural analysis enables a better representation of the true post-crack behavior and thus yielding more accurate deflection, crack width and stress distribution predictions. This results in better estimates of structure performance, especially for the members under the flexural tension and biaxial loading condition. The stress strain curve of Collins-Mitchell Model for concrete in tension is illustrated in Fig. (4).

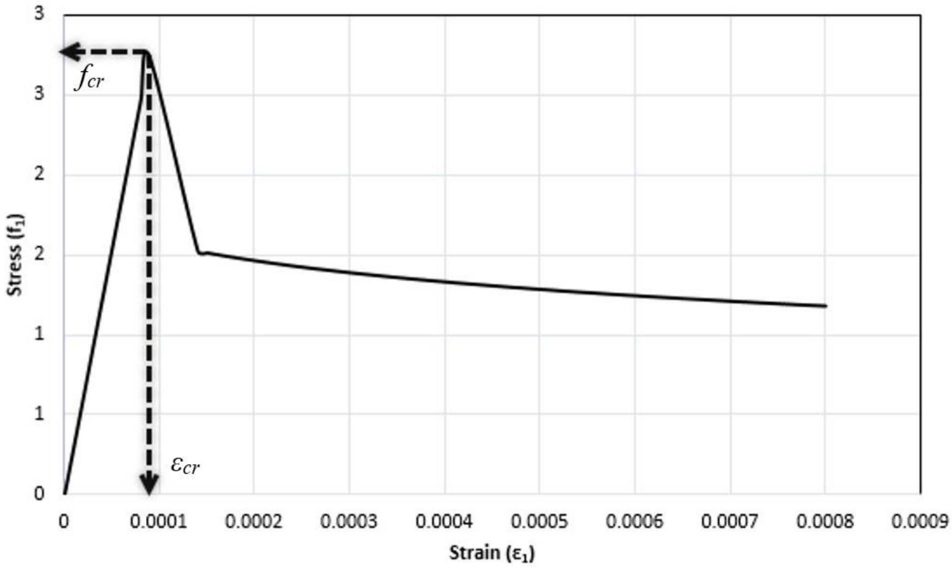

Fig. 4. Stress-strain relationship of concrete in tension using Collins-Mitchell Model

3.5 Reinforcing Steel Material Model

The Giuffre-Menegotto-Pinto model is one of the well-known constitutive models to be used for representing the nonlinear stress-strain relationship of reinforcement steel in RC structures. It represents the material behavior by a smooth and continuous curve which accounts for chronological elastic and plastic stages.

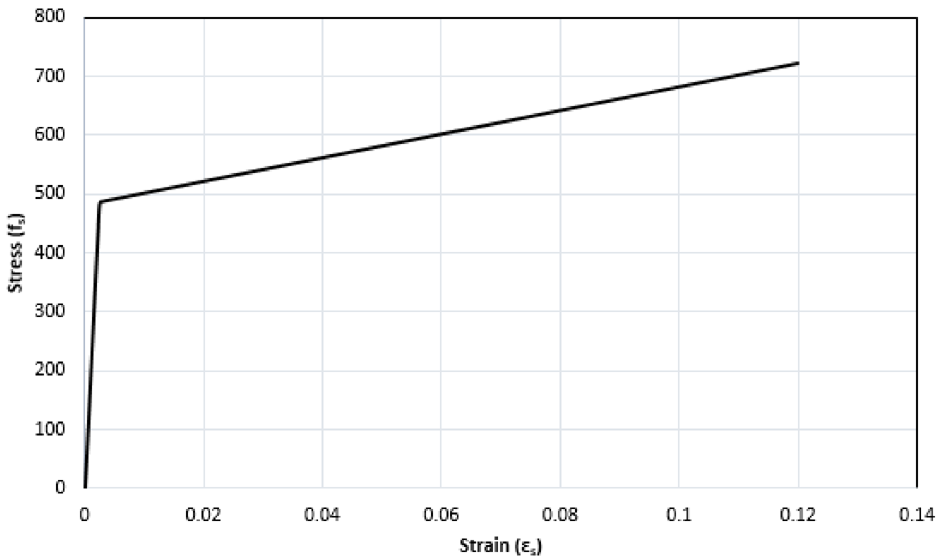

Fig. 5. Stress-strain relationship of steel reinforcement using Giuffre-Menegotto-Pinto model

First, the model is based on a relationship of linear elasticity, i.e., stress is proportional to strain (Eq. (7)), with proportionality constant being steel's modulus of elasticity. Once the material has achieved its yield point, it is said to have entered the plastic region and stress will still increase but by a decreasing amount. In this stage, the material response is given by Eq. (8).

$$f_s = E_0 * \varepsilon_s, for\ f_s \leq f_y \tag{7}$$

$$f_s = f_y + b * E_0 * \varepsilon_s, for\ f_s \geq f_y \tag{8}$$

Where; E_0 Initial elastic modulus of steel reinforcement, b Ratio between post-yield tangent and elastic tangent, ε_s Strain occurring in steel reinforcement, f_s Stress acting on steel reinforcement, f_y Stress at yielding of steel reinforcement.

4. Validation of Experimental Results

To validate the results of NLFEA obtained during this study, previous experimental results were used. Several experimental programs of concrete members under simultaneous flexure and temperature loadings were examined and according to their relevance, level of accuracy as well as accordance with the modelling approach used in this study. By comparing the predicted response of the structure from the NLFEA in terms of load–displacement curves, and crack patterns with previous experimental results, it is possible to assess thoroughly the reliability and prediction capabilities of such numerical models. Details of the key experimental results were previously summarized in this paper. It is also detailed how these have been used to validate the NLFEA results in the following sections.

4.1 Validation of NLFEA Against Experimental Results by DeRosa et al.

The loading sequence applied was divided into four stages, each stage consisting of specific steps. In the initial stage (Step (1)), a monotonic load was applied. This load increased successively from 0 kN to 75 kN. In the second stage (Step (2)), a sustained constant load of 75 kN was applied. The second step for beam (1) and beam (2) is that the ambient temperature drops to (-20^{0}C). For the subsequent 10 steps (steps 3 to 12), the model experienced a 10-cycle load history. Each cycle comprised alternating loads of 75 kN – 50 kN was then exerted as the compliance for this kind of continuous wave test on air bearings. To evaluate cyclic behavior. Last, in step (13), the final step involved a monotonic loading phase. Starting from 75 kN, the load was increased to failure. This made it possible to evaluate ultimate load capacity. Materials properties for both concrete and reinforcing steel in the numerical modelling were defined based on information from DeRosa et al. [8]. They are given in Table (4). These properties were incorporated to guarantee the same behavior of specimens both under NLFEA simulation for comparison with actual structural test results where necessary. Relevant concrete parameters included compressive strength, tensile strength and E/P ratio. Certain reinforcing steel properties such as yield strength, ultimate strength and E were also defined. These input values guaranteed a capable foundation for studying structural reaction under the thermal and mechanical loads. Fig. (6) displays the temperature loading stage in NLFEA.

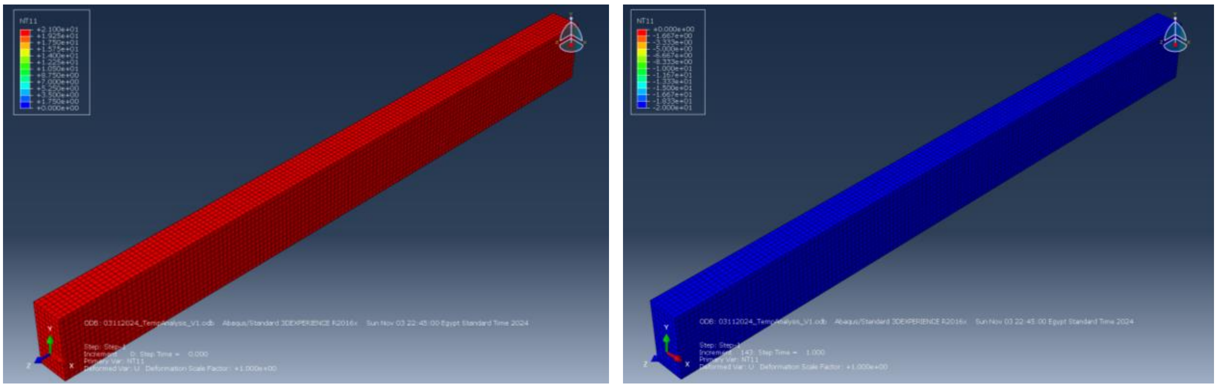

(a) (b)

Fig. 6. (a) Initial Ambient Temperature surrounding RC Beam (Step 1), (b) Final Ambient Temperature surrounding RC Beam (Step 2)

Fig. (7) displays load-displacement behavior alongside concrete cracking. Through calculations, the NLFEA results show good agreement with data from experimentations. It really confirms that the incorporated modeling approach is accurate. Fig. (7) validates the effectiveness of NLFEA in simulating complicated behavior by such concrete members when simultaneously subjected to both temperature and gravity loadings.

Table 4. Material properties of reinforcing steel and concrete of DeRosa et al. [8] specimens

Material Property	Reinforcing Steel		Concrete
	10 M	20 M	
Modulus of elasticity (MPa)	200000	200000	28200
Poisson's ratio	0.30	0.30	0.18
Yield strength (MPa)	478	453	NA
Ultimate Strength (MPa)	576	563	NA
Compressive strength (MPa)	NA	NA	36
Density (kg/m³)	7850	7850	2400
Coefficient of thermal expansion (/⁰C)	$12*10^{-6}$	$12*10^{-6}$	$10*10^{-6}$

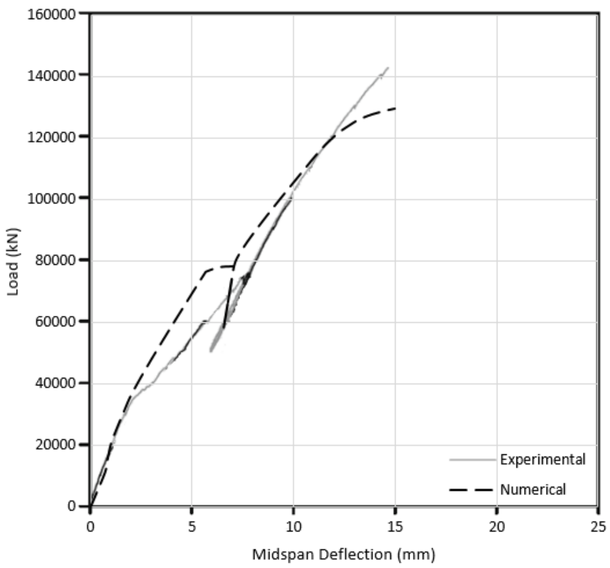

(a) Beam (1)

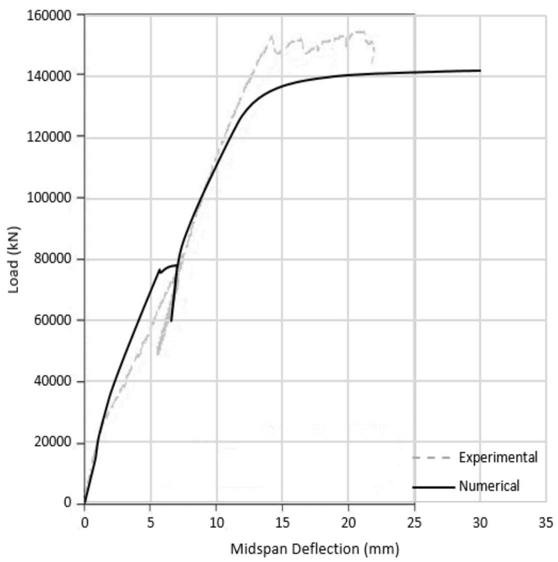

(b) Beam (2)

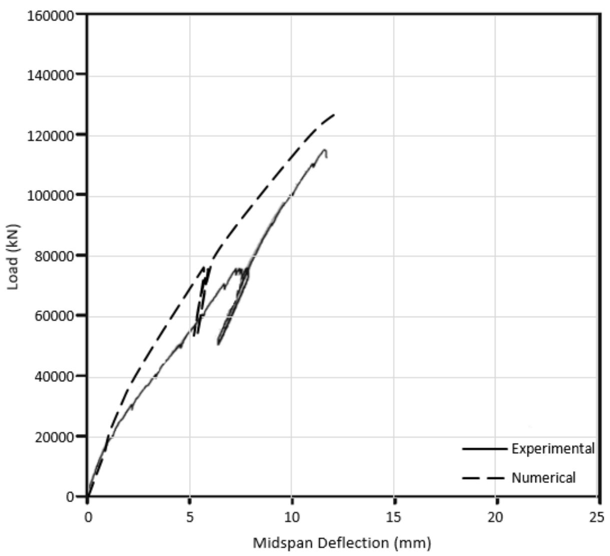

(c) Beam (3)

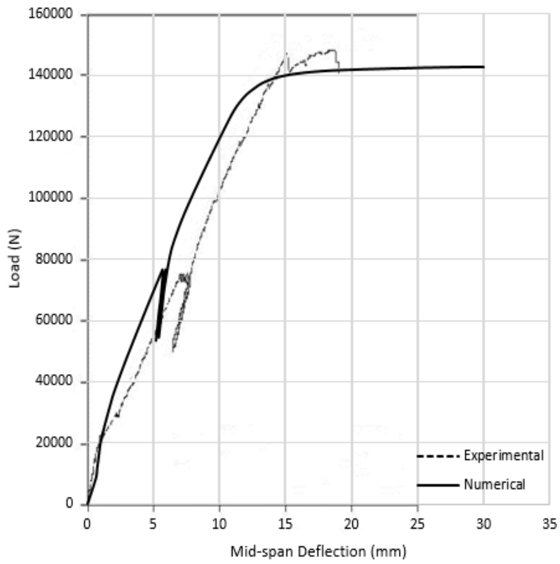

(d) Beam (4)

Fig. 7. Load-displacement relationship DeRosa et al. [8] specimens

4.2 Validation of NLFEA Against Experimental Results by Mirzazadeh et al.

The loading procedure was split into four distinct steps. In Step (1), load was incrementally applied and rose from 0 to 90 kN. In step (2), a sustained constant load of 90 kN was applied. During second step, temperature decreased in ambient temperature for beam (WSL) and beam (NSL), as illustrated in the Fig. (8). For the next 10 steps (i.e., from step 3 to step 12), the beam was loaded to 90 kN, then back to 50 kN after pulling in each loading cycle and finally to 75 kN, in order to investigate the cyclic behaviour of the material. Finally, step (13) was a monotonic loading from 90 kN to failure which could be used as a measure of the ultimate carrying capacity of the beam.

ABAQUS/CAE was used to define the material properties of the two materials, concrete and reinforcing steel. The experimental data comes from Mirzazadeh et al. [9] and is summarized in Table (5). Thus, these parameters should ensure that both NLFEA and experimental results yield matching results. Compressive strength, splitting tensile strength, elastic, and Poisson's ratio are the principal inputs. Both elastic modulus and Poisson's Ratio affect the deformation of materials with respect to time. The performance of these reinforcing bars is described using its ultimate strength, yield point and Young's modulus of elasticity. Fig. (8) indicates the results of temperature-gradient applied on RC beam during experimental testing. Results of the NLFEA are shown in Fig. (9). These figures show how the RC beams responded to different loading conditions, with critical parameters such as load-displacement relationship, cracking pattern and stress distribution. The numerical results showed strong agreement with the experimental results. This confirms the accuracy of the modelling approach.

Table 5. Material properties of reinforcing steel and concrete of Mirzazadeh et al. [9] specimens

Material Property	Reinforcing Steel		Concrete
	10 M	20 M	
Modulus of elasticity (MPa)	200000	200000	30820
Poisson's ratio	0.30	0.30	0.18
Yield strength (MPa)	481	421	NA
Ultimate Strength (MPa)	669	531	NA
Compressive strength (MPa)	NA	NA	43
Density (kg/m^3)	7850	7850	2400
Coefficient of thermal expansion (/^{0}C)	12*10^{-6}	12*10^{-6}	10*10^{-6}

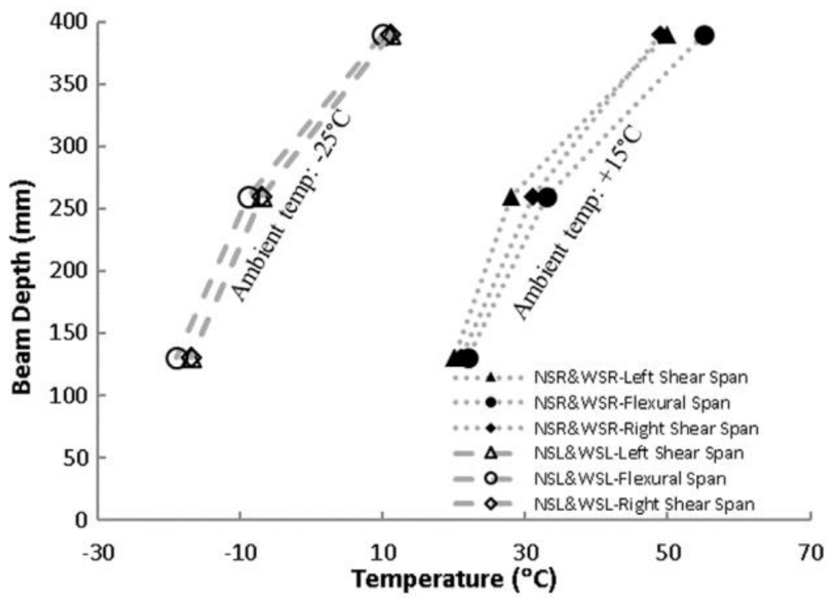

Fig. 8. Thermal gradient over the depth of the beams during tests

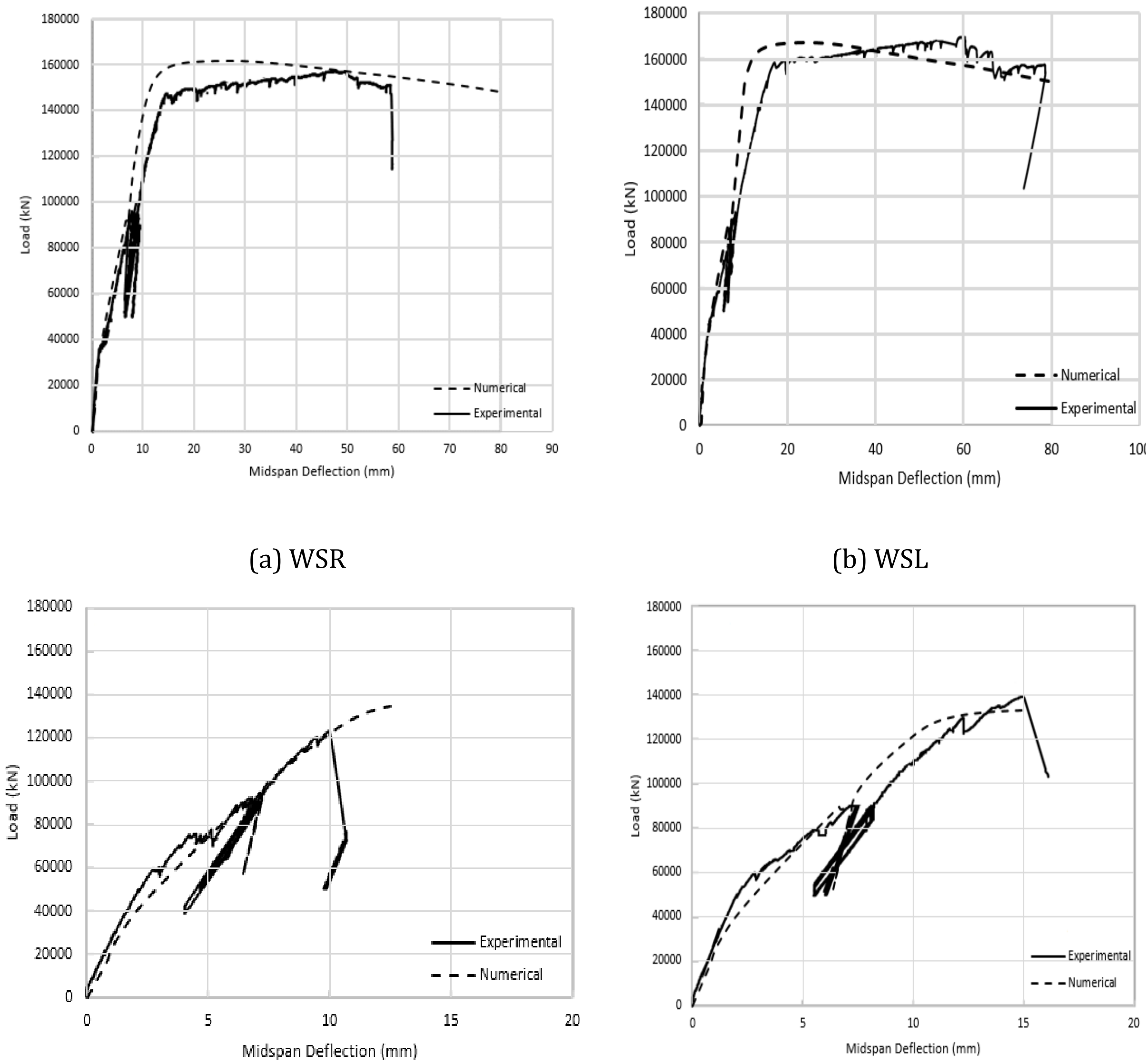

(a) WSR (b) WSL

(c) NSR (d) NSL

Fig. 9. Load-displacement relationship for Mirzazadeh et al. [9] specimens

4.3 Mesh Sensitivity Analysis

Mesh sensitivity refers to the impact of mesh size and quality on the accuracy of numerical predictions. Lower resolution meshes typically yield more accurate results but also increase computational cost. Sparse number of mesh elements lowers computer resource requirements but can sacrifice precision. To obtain reliable simulations at a reasonable cost, the balance between mesh size is important. Mesh supports the optimization of this balance, by allowing elements sizes to be modified according to error estimates. Mesh sensitivity is an important aspect for accurate and efficient simulations in engineering and scientific programs. The results provided in Fig. (10) with mesh sensitivity analysis reveals load-deflection curves of RC Beam (4) for M30, M40, M50 and M60 compared to experimental results. As the mesh becomes finer (from M60 to M30), NLFEA predictions are in better agreement and nearer to the experimental curve, particularly so on the ascending limb and close to the peak load. The quantification of initial stiffness and peak load for coarser meshes. M60 underestimates them; however, finer meshes (M30, M40) result in more reliable and stable results. Past the peak, all models fit the decrease in trend, but with varying amounts of smoothness. Regarding the mesh convergence of the presented results, M30, M40, and M50 are in agreement indicating increased independence at finer resolutions.

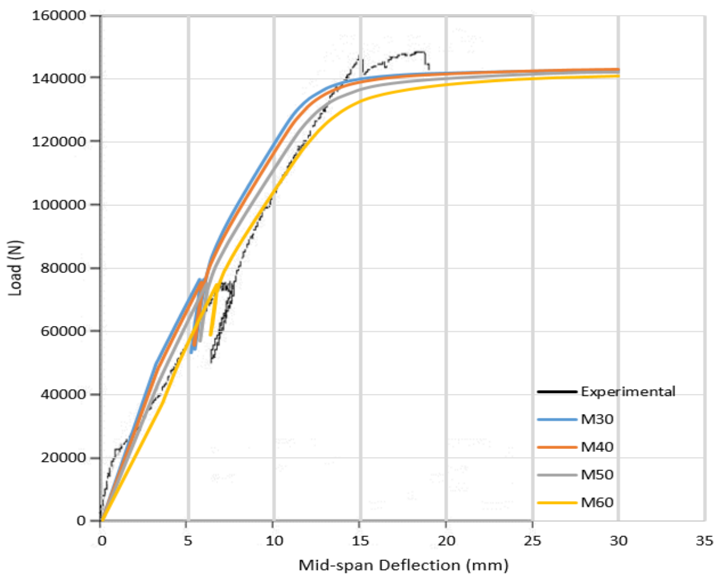

Fig. 10. Mesh sensitivity analysis carried out for Beam (4)

5. Results and Discussion

A comparison of test results and NLFEA predictions for the four RC beams tested by DeRosa et al. is summarized in Table (6). Generally, NLFEA tended to slightly over-predict the cracking loads, such as Beam 1 39kN vs. 36kN, with difference +8.3%. It also tended to underestimate the ultimate capacities, such as Beam 2 142kN vs. 153kN, with difference −6.5%. For all other beams similar minor deviations, but still within acceptable limits, were observed. In general, NLFEA-based method gave fairly accurate predictions for both cracking behavior and ultimate strength, with margin of error within 10%, hence confirming the reliability of such approach for this type of analysis.

Table 6. Comparison between experimental and NLFEA results for DeRosa et al. [8] specimens

Beam No.	Experimental Cracking Load (kN)	NLFEA Cracking Load (kN)	Difference (%)	Experimental Ultimate Load (kN)	NLFEA Ultimate Load (kN)	Difference (%)
1	36	39	8.33	142	130	-8.45
2	30	33	10.00	153	142	-6.54
3	30	28	-6.67	128	126	-1.56
4	24	25	4.17	149	142	-4.70

Table7. Comparison between experimental and NLFEA results for Mirzazadeh et al. [9] specimens

Beam ID	Experimental Cracking Load (kN)	NLFEA Cracking Load (kN)	Difference (%)	Experimental Ultimate Load (kN)	NLFEA Ultimate Load (kN)	Difference (%)
WSR	36	39	8.33	157	161	2.54
WSL	48	51	6.25	169	168	-0.60
NSR	60	52	-13.33	123	135	9.76
NSL	56	52	-7.14	139	133	-4.32

A comparison with the four RC beams tested by Mirzazadeh et al. is presented in Table (7). In general, the NLFEA results were in excellent agreement with the experimental data. For instance, the Beam WSR was also in good agreement with cracking load (+8.3%) and ultimate strength (+2.5%), and that for the Beam WSL was also in a reasonable point (cracking load +6.3%, ultimate, with difference −0.6%). For Beams NSR and NSL, larger discrepancies were found, with underpredictions of the cracking load (−13.3% and −7.1%, respectively) but overpredictions or very small reductions for the ultimate strength. In consideration of these discrepancies, however, the NLFEA method was in reasonable agreement with cracking mode and ultimate capacity.

The comparison between the experimental load-displacement responses and those provided by NLFEA reveals an overall satisfactory agreement, with margin of error within 10%. Thereby validating the numerical model as far as it concerns the response of the structure at global level. The experimental results show evident residual deformation due to the cyclic loading conditions applied. This indicates irreversibility of the resistances accompanying crack formation in concrete and yielding of steel and accumulated damage. These residual deformations are less significant in the corresponding NLFEA results, likely a result of the idealized material constitutive behavior and damage evolution inherent to the numerical framework. In addition, according to the numerical simulations, stiffer behavior was noticed as compared to experimental results. Such a small difference in the stiffness may be attributed to mainly using the cyclic loading in the experimental tests, which leads to progressive stiffness degradation and micro-cracking phenomena of which are only partially represented within the numerical model. In general, such minor differences, good agreement between the NLFEA and experimental responses, show that the proposed developed NLFEA technique is reliable in terms of simulating complex behavior under combined loading. In general, the NLFEA predictions were well correlated with experimental data and particularly in ultimate load prediction. More variation in predicting cracking loads occurred, possibly due to sensitivity towards modeling assumptions with respect to tension stiffening and initial cracking response. However, the NLFEA model was successful in predicting the structural behavior of the RC beams subjected to the loading condition used in this study.

6. Conclusions

The thermo-mechanical response of RC members under combined gravity and temperature loading was analyzed in this study, based on a developed NLFEA approach. The numerical results demonstrate that temperature affect strongly the cracking initiation, stiffness softening and ultimate load-carrying capacity. Thus, volumetric changes need to be taken explicitly into account in structural analysis. Validation with experimental results of RC beams subjected to uniform temperature changes and through-depth temperature differences showed a efficient correlation between NLFEA results and test results. Cracking loads were in general overestimated by about 6–9% but ultimate capacities had some underestimation; however, with differences of an order of only 7% on average. The maximum error between simulation and experiment was less than 10% for all specimens tested. The load–displacement curves, initial stiffness, peak forces, post peak softening and observed cracking patterns were correctly captured by the NLFEA demonstrating a consistent description of structural response to coupled thermal and mechanical loading.

The outcomes of NLFEA demonstrate the necessity of including the concrete material nonlinearity including tension stiffening and stiffness degradation by using model in conjunction with modified Hognestad stress–strain relationship. The explicit inclusion of the differential thermal expansion between steel reinforcement and concrete was found to be essential for producing realistic internal stress states and crack propagation behavior. Mesh sensitivity analyses additionally substantiated numerical convergence, as smaller thicknesses (M30–M40) yielded stable and accurate predictions. The incorporation of the latest modulus of rupture expression from ACI 318-25 resulted in better estimates for cracking load, as compared to earlier code expressions. The proposed NLFEA framework affords a strong foundation for subsequent parametric studies to quantify the interaction of volumetric changes and gravity loads. Such findings may fill some existing gaps for influencing temperature load effects in the international design codes. The results also indicate calibrated linear finite element methods could be established to achieve NLFEA accuracies for practical designs. Such a complementary approach would make structural analysis more reliable and promote wider application and practicability of temperature-induced design provisions in engineering practice.

References

[1] Vecchio FJ. Nonlinear Analysis of Reinforced Concrete Frames Subjected. ACI Struct J. 1987;84:492-501.

[2] Vecchio FJ, Agostino N, Angelakos B. Reinforced concrete slabs subjected to volumetric changes. Can J Civ Eng. 1993;20(5):741-753. https://doi.org/10.1139/l93-099

[3] Ariyawardena N, Ghali A, Elbadry M. Experimental study on thermal cracking in reinforced concrete members. ACI Struct J. 1997;94(4):432-441. https://doi.org/10.14359/494

[4] Elbadry M, Ghali A. Thermal stresses and cracking of concrete bridges. In: J Proc. 1986;83(6):1001-1009. https://doi.org/10.14359/2670

[5] Elbadry M, Ghali A. Control of thermal cracking of concrete structures. ACI Struct J. 1995;92(4):435-450. https://doi.org/10.14359/993

[6] Ghali A, Favre R, Elbadry M. Concrete structures: Stresses and deformations: Analysis and design for serviceability. CRC Press; 2018. https://doi.org/10.1201/9781482289138

[7] Do TMD, Lam TQK, Van Thuc N. Analysis of axial stiffness reduction factors in thermal analysis of multistorey buildings. In: IOP Conf Ser Mater Sci Eng. 2020;988(1):012059. https://doi.org/10.1088/1757-899X/988/1/012059

[8] DeRosa D, Hoult NA, Green MF. Effects of varying temperature on the performance of reinforced concrete. Mater Struct. 2015;48:1109-1123. https://doi.org/10.1617/s11527-013-0218-y

[9] Mirzazadeh MM, Noël M, Green MF. Effects of low temperature on the static behaviour of reinforced concrete beams with temperature differentials. Constr Build Mater. 2016;112:191-201. https://doi.org/10.1016/j.conbuildmat.2016.02.216

[10] Collins MP, Mitchell D. Prestressed concrete structures. Response Publications; 1997.

[11] El-Tayeb EH, El-Metwally SE, Askar HS, Yousef AM. Thermal analysis of reinforced concrete beams and frames. HBRC J. 2017;13(1):8-24. https://doi.org/10.1016/j.hbrcj.2015.02.001

[12] Pooja M, Karthiyaini S. Investigation of flat slab structures with and without expansion joints for thermal stresses. Int J Civ Eng Technol. 2017;8:1287-1295.

[13] Hisham A, Mahmoud GH, Nasr NE, Mohamed A, Rahim A. Finite Element Modelling of Structures Subjected to Thermal Loading. IOSR Journal of Mechanical and Civil Engineering (IOSR-JMCE.2018:15(6): 31-43

[14] Hisham A, Turk BS, Nasr NE, Goda HA. Assessment of Flat Slab Axial Stiffness in Thermal Analysis. Al-Azhar University Civil Engineering Research Magazine. 2022: 44(1):133-158

[15] Ahmed K. Temperature effects in multi-story buildings. JES J Eng Sci. 2011;39(2):249-267. https://doi.org/10.21608/jesaun.2011.120405

[16] Systèmes D. Abaqus analysis user's manual. Simulia Corp. Providence, RI, USA. 2007;671(40):672.

[17] American Concrete Institute, ACI Committee 224. Control of Cracking in Concrete Structures (ACI 224R-01). American Concrete Institute-ACI; 2001.

[18] American Concrete Institute. Building Code Requirements for Structural Concrete (ACI 318-25) and Commentary. American Concrete Institute; 2025.

[19] European Committee for Standardization (CEN). Eurocode 2: Design of concrete structures - Part 1-1: General rules and rules for buildings (EN 1992-1-1). CEN; 2004.

[20] British Standard. Eurocode 8: Design of structures for earthquake resistance (BS EN 1998-1). 2005.

[21] ECP Committee. Egyptian Code for Design and Construction of Concrete Structures (ECP 203-2025). Cairo, Egypt: Housing and Building National Research Center; 2025.

[22] ACI Committee 435. Control of deflection in concrete structures (ACI 435R-95) (Reapproved 2000). American Concrete Institute; 2000.

[23] Hognestad E. A study on combined bending and axial load in reinforced concrete members (Report No. 399). University of Illinois Engineering Experiment Station; 1951.

[24] Lubliner J, Oliver J, Oller S, Onate E. A plastic-damage model for concrete. Int J Solids Struct. 1989;25(3):299-326. https://doi.org/10.1016/0020-7683(89)90050-4